56 GBaud PAM-4 Direct Detection with High-Speed Avalanche Photodiodes

Tobias Beckerwerth[1], Christoph Kottke[1], Volker Jungnickel[1], Ute Tropenz[1], Martin Möhrle[1], Patrick Runge[1], Martin Schell[1,2]

[1]Fraunhofer Heinrich Hertz Institute, Einsteinufer 37, 10587 Berlin, Germany
[2]Technical University Berlin, 10623 Berlin, Germany
Author e-mail address: tobias.beckerwerth@hhi.fraunhofer.de

Abstract: We demonstrate 56 GBaud PAM-4 transmission by using a high-speed waveguide avalanche photodiode (WG APD) and an electro absorption modulated laser (EML). Compared to a PIN photodiode, the WG APD reduces the power budget in a B2B setup by 6 dB.

1. Introduction

Driven by the demand for cloud services, today's internet traffic is dominated by inter- and intra-data center transmission with distances up to 80 km. Although coherent systems are expanding to cover inter-data center transmission below 80 km [1], short-reach intra-data center traffic up to 2 km is mainly realized by intensity modulated direct detection (IM/DD) in the O- and C-band [2,3]. To address the resulting challenges of high capacity data center interconnections (DCI), high performance photonics with low power consumption are mandatory. Enhancement of receiver sensitivity reduces the required laser power and thus a large share of overall power consumption incurred by driving and cooling the transmitting laser.

We present an evanescent coupling high-speed waveguide integrated avalanche photodiode (WG APD) showing high bandwidth up to 37 GHz operating at bias voltages below 20 V. Applied with an electro-absorption modulated laser (EML) in a simplified setup for 56 GBaud PAM-4 direct detection, the WG APD enables 20 km transmission and a reduces the power budget by 1.5 dB. The reduction of the power penalty increases at shorter distances and can leverage the overall power consumption in DCI.

2. APD Design and Performance

For 56 GBaud PAM-4 detection, linearity and bandwidth are essential design parameters. Additionally, a high intrinsic responsivity enables a high sensitivity and an increased transmission distance at a given power budget. By integrating the avalanche photodiode on an evanescent coupling waveguide structure, a WG APD can fulfill these requirements, due to a relaxed trade-off between sensitivity and bandwidth compared to vertically illuminated photodiodes. Further, evanescent WG APDs can be monolithically integrated with other components [4] and allow a simplified fabrication compared to butt-joint coupled devices [5].

The presented WG APD extends the conventional concept with separated absorption, charge, and multiplication (SACM) layer design [6] with an additional charge (C) and InAlAs transit (T) layer. This sophisticated epitaxial SACMCT structure minimizes the depleted absorbing region (see Fig. 1a) without sacrificing the RC limitation of the device. By an undepleted absorber, the holes carrier transit time is minimized. As a drawback, this leads to an increased RC time constant, which is determined by the depleted regions of the photodiode. To overcome the RC limitation, the APDs capacitance is lowered by the InAlAs transit region similar to the collection layer in uni-travelling carrier photodiodes [7]. Compared to current state-of-the-art APDs, we achieve similar performance regarding the responsivity and bandwidth [6]. As against other waveguide integrated devices, the demonstrated WG APD shows slightly lower gain [5, 8], but also a lower dark current to enhance the receiver sensitivity.

a)

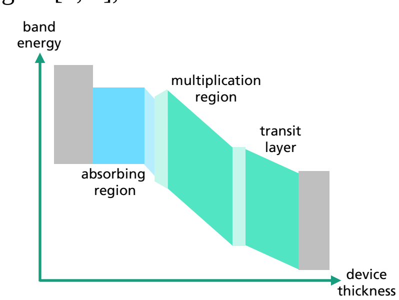

b)

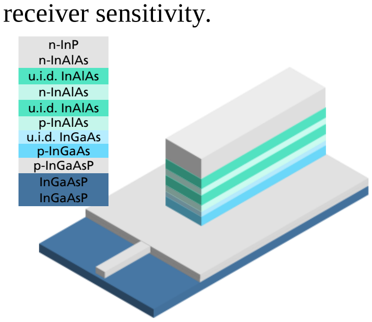

Fig. 1. Epitaxial layer structure (a) and band diagram (b) of the sophisticated SACMCT waveguide integrated APD

To optimize the quantum efficiency of the evanescent coupling structure, the APD structure is placed with the p-contact above the waveguide layers, rather than the n-contact at the bottom [4,5]. This leads to an increasing refractive index profile from the waveguide layer to the thin absorbing region and thus avoids optical coupling through the transparent multiplication region (see Fig. 1b). As a result, the device demonstrates high-speed performance compatible for 56 GBaud PAM-4 operation with an enhanced sensitivity. The external responsivity at the unity gain voltage (7 V), the IV and gain characteristics (M), as well as the small-signal parameters at different bias voltages are shown in Fig. 2.

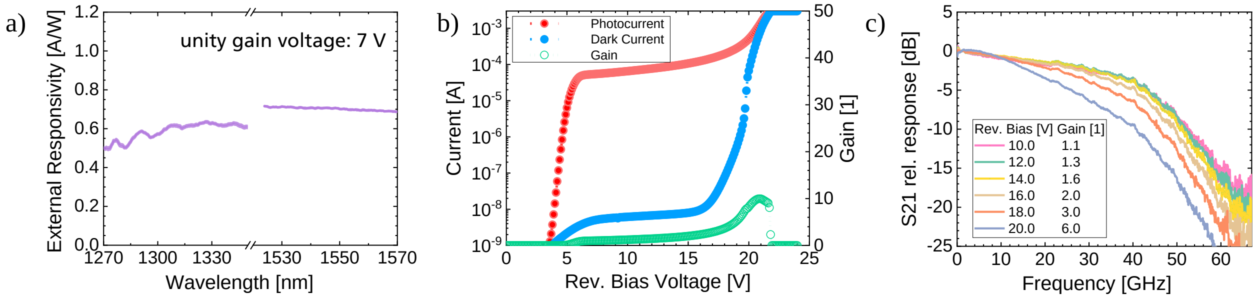

Fig. 2. External responsivity at unity gain (a), IV characteristics (b), S21 small-signal parameters (c) of the fabricated WG APD

At the unity gain voltage of 7 V our device shows a high responsivity of > 0.5 A/W and > 0.65 A/W in the O-band and C-band, respectively. The IV characteristics show a moderate gain up to M=2 and a low dark current below 10 nA at a reverse bias voltage of 16 V. When increasing the reverse bias from 18 V to 19 V, the gain increases from M=3 to M=4, while the dark current remains below 1 µA. The maximum 3dB-bandwidth is 37 GHz for a voltage up to 14 V at a gain of M=1.6 and reduces to 30 GHz when increasing the reverse bias to 16 V (see Fig. 2).

3. System Evaluation

The WG APD is investigated in a simplified setup for direct detection, using an EML driven by a 265 Gs/s AWG for 56 GBaud PAM-4 signal generation. The components are connected by a standard single mode fiber supplemented by a praseodymium-doped amplifier, and a variable optical attenuator. The received signal is amplified and fed to a 256 GS/s oscilloscope, or a digital-to-analog converter, respectively (see Fig. 3a). The digital signal processing consists of pulse shaping with roll-off 1 and linear equalization at the Rx.

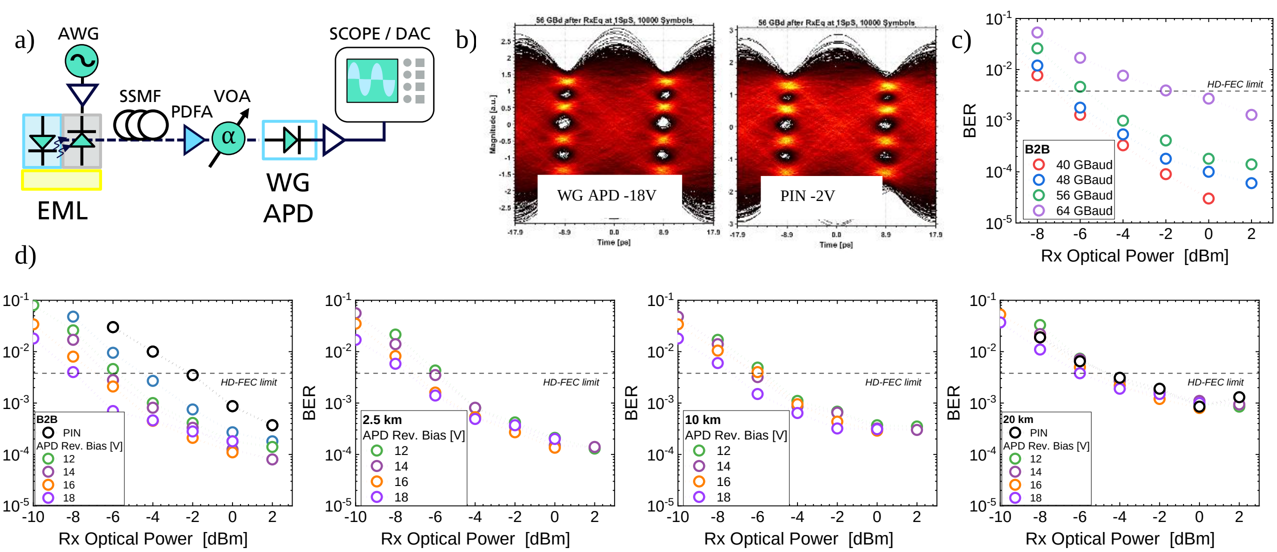

Fig. 3. System setup (a), eye diagrams in B2B configuration of PIN and WG APD (b) and measurement results of BER for different baud rates (c) and the evaluation of a the WG APD in 56 GBaud PAM-4 transmission (d). EML: electro absorption modulated laser, AWG: arbitrary waveform generator, SSMF: standard singe mode fiber, PDFA: praseodymium-doped fiber amplifier, VOA: variable optical attenuator, WG APD: waveguide avalanche photodiode, SCOPE/DAC: oscilloscope / digital-analog converter

For the generation of 56 GBaud PAM-4 signals, the InP-based EML module [9] is driven at laser current of 100 mA emitting at the wavelength of 1290 nm. The applied reverse bias voltage at the electro-absorption modulator is set to -1.1 V and a modulation swing of V_{pp}=300 mV is applied for all further investigations. A thermoelectric cooler (TEC) keeps the temperature at 45°C. To prove the setup, clear eyes were obtained at an Rx optical power of 0 dBm employing the WG APD at a reverse bias of 18 V respectively the PIN photodiode at 2 V (Fig. 3b).

To evaluate 56 GBaud PAM-4 operation, the WG APD is applied in a back-to-back (B2B) experiment. We find a BER below the FEC limit of $3.8x10^{-3}$ for receiver Rx optical powers above -7.2 dBm, -6.8 dBm and -5.8 dBm for symbol rates of 40 GBaud, 48 GBaud and 56 GBaud, respectively. At a symbol rate of 64 GBaud, the minimum optical input power increases significantly to 2 dBm due to the limiting bandwidth of the WG APD (Fig. 3c). Further, we determined the BER for different transmission distances between 0 km and 20 km at various reverse bias voltages between 12 V and 18 V according to gain characteristics covering M=1.3 to M=3 by varying the optical Rx optical power. The BER is minimized at the maximum Rx power of 2 dBm for all different transmission distances. However, in the B2B scenario, the BER slightly increases when the optical power is decreasing. For distances of 2.5 km and beyond, the BER is barely changing for Rx optical powers between 0 dBm to 2 dBm, proving that the error-floor is independent from the received power (see Fig. 3d). This effect occurs for the PIN photodiode as well as for all applied reverse bias voltages at the WG APD. We conclude that this effect is resulting from the signal dispersion at 1290 nm caused by the EML. Still, the error-floor for each investigated transmission distance is below the FEC limit, making the setup suitable for transmission distances up to 20 km. For the B2B setup, the resulting reduction of the power penalty at the FEC threshold is 6 dB. However, this reduced power penalty compared to using a PIN photodiode instead of the WG APD decreases with the transmission distance due to dispersion. At the maximum investigated distance of 20 km, the minimum Rx power to receive a BER below the FEC is -4.5 dBm for the PIN photodiode and -5.9 dBm for the WG APD, translating to a reduction in the power penalty of 1.5 dB.

4. Conclusion

We demonstrated a novel WG APD with 37 GHz 3dB-bandwidth operating from O- to C-band. The WG APD with an EML as transmitter are analyzed regarding 56 GBaud PAM-4 transmission. In a B2B scenario, the WG APD reduces the power budget by 6 dB. This advantage reduces for longer transmission distances to still 1.5 dB at 20 km.

Both, the WG APD as well as the EML can be fabricated in an array configuration [10], allowing for LAN-WDM operation. Further, using the WG APD on the receiver with a minimum Rx optical power of -5.9 dBm, the optical EML output power of 3.5 dBm is sufficient to allow 20 km transmission at a total power budget of 9.4 dB. Conclusively, the demonstrated performance can enable the deployment of DCI for short-reach transmission according to 400 Gb/s IEEE standardization [11].

[1] D. Tauber, "Role of Coherent System in the Next DCI Generation," in *2022 Optical Fiber Communications Conference and Exhibition (OFC)*, 2022, p. M1D.1, doi: 10.1364/ofc.2022.m1d.1.

[2] X. Pang *et al.*, "Short Reach Communication Technologies for Client-Side Optics beyond 400 Gbps," *IEEE Photonics Technol. Lett.*, vol. 33, no. 18, pp. 1046–1049, 2021, doi: 10.1109/LPT.2021.3078255.

[3] J. Zhang *et al.*, "Demonstration of 100-Gb/s/λ PAM-4 TDM-PON supporting 29-dB power budget with 50-km reach using 10G-class O-band DML transmitters," in *2019 Optical Fiber Communications Conference and Exhibition (OFC)*, 2019, p. Th4C.3, doi: 10.1364/ofc.2019.th4c.3.

[4] T. Beckerwerth, R. Behrends, F. Ganzer, P. Runge, and M. Schell, "Linearity Characteristics of Avalanche Photodiodes for InP Based PICs," *IEEE J. Sel. Top. Quantum Electron.*, vol. 28, no. 2, pp. 1–8, 2022, doi: 10.1109/JSTQE.2021.3127853.

[5] T. Okimoto *et al.*, "106-Gb/s Waveguide AlInAs/GaInAs Avalanche Photodiode with Butt-joint Coupling Structure," in *2022 Optical Fiber Communications Conference and Exhibition (OFC)*, 2022, p. W3D.2, doi: 10.1364/ofc.2022.w3d.2.

[6] M. Nada, T. Yoshimatsu, F. Nakajima, K. Sano, and H. Matsuzaki, "A 42-GHz bandwidth avalanche photodiodes based on III-V compounds for 106-Gbit/s PAM4 applications," *J. Light. Technol.*, vol. 37, no. 2, pp. 260–265, 2019, doi: 10.1109/JLT.2018.2871508.

[7] T. Beckerwerth, P. Runge, H. Boerma, F. Ganzer, and M. Schell, "High-Speed Waveguide Integrated Avalanche Photodiode for InP-PICs," in *IEEE Photonics Conference*, 2022, p. TuA2.2.

[8] M. Huang, K. Lee, K. Magruder, O. Dosunmu, and R. Haislmaier, "200Gb / s per lane Ge / Si waveguide avalanche photodiode," in *European Conference on Optical Communication (ECOC)*, 2022, no. 1, p. Th2E.2.

[9] P. Runge *et al.*, "InP-components for 100 gbaud optical data center communication," *Photonics*, vol. 8, no. 1, pp. 1–10, 2021, doi: 10.3390/photonics8010018.

[10] M. Theurer *et al.*, "4 × 56 Gb/s High Output Power Electroabsorption Modulated Laser Array with up to 7 km Fiber Transmission in L-Band," *J. Light. Technol.*, vol. 36, no. 2, pp. 181–186, 2018, doi: 10.1109/JLT.2017.2750764.

[11] IEEE P802.3bs, "400 Gb/s ethernet task force," *https://www.ieee802.org/3/bs/*, 2016. https://www.ieee802.org/3/bs/.